Experiments in Fluids 33 (2002) 346–350
DOI 10.1007/s00348-002-0446-3

Flow over convergent and divergent wall riblets

K. Koeltzsch, A. Dinkelacker, R. Grundmann

Abstract Fast swimming sharks have small riblets on their skin, which are assumed to improve the swimming performance of the fish. Fluid dynamic experiments in water as well as in air confirm this assumption. With riblet surfaces as compared to smooth surfaces, drag reductions up to about 10% were measured. The overall riblet pattern on sharks shows parallel riblets directed from head to tail, but besides this overall pattern fast swimming sharks have also small areas with converging riblets and others with diverging riblets. In the present study the velocity field over convergent and divergent riblet patterns is investigated by hot-wire measurements in turbulent pipe flow. Significant changes in the near wall velocity field were found.

1 Introduction

It is known that skin friction can be reduced by using fine riblets lying in the flow direction on the wall instead of a smooth surface (e.g., Walsh and Weinstein 1978; Reif and Dinkelacker 1982; Bechert et al. 1985). A review is given by Walsh (1990). Bechert et al. (1997) carried out extensive investigations dealing with the size of riblets, the optimal cross-sectional shapes, and the ratio of riblet spacing s to riblet height h. Blade riblets, which are thin plates aligned in the flow direction and perpendicular to the wall, seem to be the optimal design. Drag reduction of almost 10% appears at an optimal ratio of riblet spacing to riblet height $s/h \cong 2$ and at $s^+ \cong 17$, where $s^+ = sU_\tau/\nu$ (where s^+ is riblet spacing in wall units, U_τ is friction velocity, and ν is the kinematic viscosity of the fluid).

Received: 21 May 2001 / Accepted: 20 March 2002
Published online: 18 June 2002

K. Koeltzsch (✉), A. Dinkelacker, R. Grundmann
Institut für Luft- und Raumfahrttechnik,
Technische Universität Dresden,
36460 Merkers, Germany
E-mail: konrad@koeltzsch.com

Present address: K. Koeltzsch
Department of Chemical Engineering,
The Ohio State University, Columbus, OH 43210-1180, USA

We would like to thank the Deutsche Forschungsgemeinschaft (DFG) for their support. This work is part of the project: "Strömungsbeeinflussung durch richtungsabhängige Wandrauhigkeit" (Flow control by directional wall roughness) – GR 1388/5-1. Furthermore, we gratefully acknowledge helpful suggestions on this paper given by the unknown referees.

Why does drag reduction occur? Close to the wall, the typical mean diameter of streamwise vortices is about $d^+=30$ expressed in wall units (Blackwelder and Eckelmann 1979; Kim et al. 1987). In the case of drag reduction $0<s^+<30$, the longitudinal vortices are larger in diameter d^+ than the riblet spacing s^+. Therefore, most streamwise vortices stay above the riblets, and the vortices touch only the tips of the riblets in contrast to the smooth wall where the friction surface is greater. In the case of drag increase $s^+>30$, the longitudinal vortices are smaller in diameter d^+ than the riblet spacing s^+. As a result, most streamwise vortices settle inside the riblet valley. These vortices interact actively with the increased wetted surface area and consequently the skin friction increases (Choi et al. 1993; Goldstein et al. 1995). Using the velocity field measurement technique (visualization and PIV) Lee and Lee (2001) confirmed this conjecture.

Furthermore, investigations have been made into wall riblets that are arranged oblique to the flow direction (Walsh 1982 from Walsh 1990; Walsh and Lindemann 1984; Savill 1986; Squire and Savill 1987; Hirschel et al. 1988; Coustols and Cousteix 1988; Coustols 1989; Gaudet 1989; Enyutin et al. 1991; Coustols and Savill 1992; Schwarz van Manen 1992; Schneider and Dinkelacker 1993; Kruse 1994; Hage et al. 1999, 2000). The yaw angle γ expresses the angle between the flow direction and the aligned riblets (see Fig. 1). The results can be summarized as follows: (1) For yaw angles γ up to 10–15° (dependent on s^+), the drag-reduction performance remains nearly unchanged. (2) The drag reduction is zero at yaw angles of about 20–35°. (3) If the yaw angle γ increases further, the skin friction also grows. (4) At a yaw angle $\gamma=90°$ (perpendicular to the riblets), the greatest value of the skin friction is obtained. This value depends on both the riblet height h^+ and the riblet spacing s^+. It should be mentioned here that for transverse grooves with ratio $s/h>10$, drag reduction is reported by Ching and Parsons (1999). Application of wall riblets in order to influence the velocity direction near the wall is discussed by Dinkelacker (1993).

In the present study, the velocity field over convergent and divergent riblet patterns was investigated by hot-wire measurements in turbulent pipe flow. This investigation was initiated by the observation of fast swimming sharks (Figs. 2 and 3). The skin of these sharks was covered with riblets, of which two areas were of interest (Dinkelacker et al. 1988): (1) The riblets converge near the so-called pit organs. Pit organs are generally regarded as sensory receptors. There is some controversy about their function in the literature. Fast swimming sharks have up to about

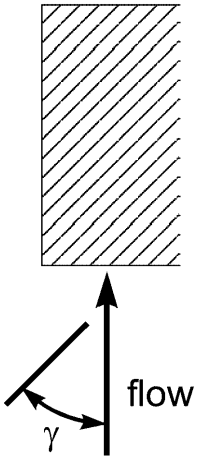

Fig. 1. Sketch of yaw angle γ between the flow direction and the aligned riblets

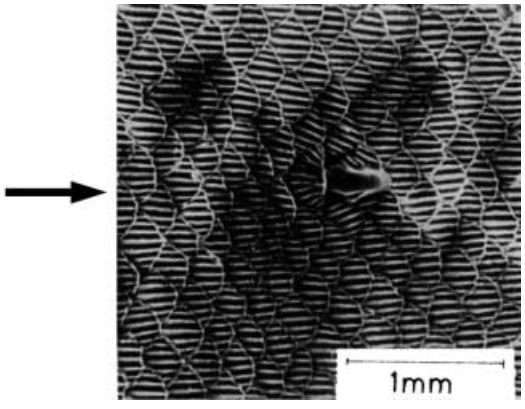

Fig. 2. Convergent riblet pattern upstream of pit organ (sensory receptor). Adult silky shark (*Carcharhinus falciformis*, length 2.27 m). Flow: left to right. Photo: W.-E. Reif, Tübingen

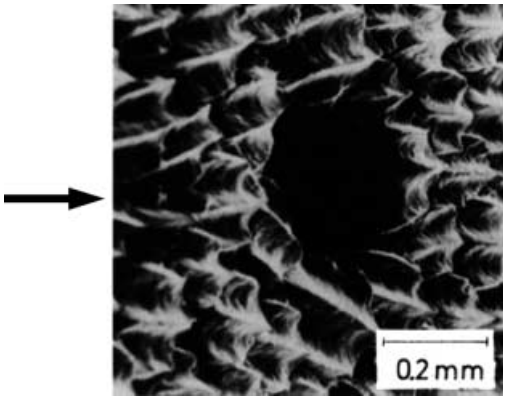

Fig. 3. Divergent riblet pattern upstream of pores of the lateral-line organ (corresponding to the human ear). Adult blue shark (*Prionace glauca*, length 2.34 m). Flow: left to right. Photo: W.-E. Reif, Tübingen

1,000 pit organs, while the number for slower sharks is smaller (Fig. 2). (2) The riblets diverge upstream of pores of the lateral-line organ (Fig. 3). This organ has some similarity to the human ear.

It should be mentioned that similar patterns (ratio of riblet spacing to riblet height s/h=10; yaw angle γ=60°) were investigated by Gao and Sunden (2001). The motivation for these investigations was the thermal and hydraulic performance of three rib-roughened rectangular ducts.

2 Experimental setup

The investigations were carried out in the laboratory of the High-Speed Wind Tunnel of the Dresden University of Technology (Germany), which is located in a salt mine 440 m under ground. The pipe channel that was used for the experiments has unusually good flow characteristics: low influence of sound and vibration from the environment, constant ambient temperature of 21°C, and a smooth pipe wall. The inner diameter is D=140 mm with a pipe length of about 38 m (see Fig. 4). Because the test section is located at about L/D=200 downstream of the pipe inlet, the turbulent pipe flow is fully developed. The centerline velocity in the channel is about U_c=56 m/s, and the Reynolds number, formed with the diameter D and the centerline velocity U_c, is about Re_D=520,000.

The experiments were performed with hot-wire measurements (constant temperature anemometry – CTA). A boundary-layer probe with a single-sensor miniature wire (DANTEC No. 55P15, 5 μm diameter , 1.25-mm long platinum-plated tungsten wire) was used to measure the velocity close to the wall. The hot-wire probe was arranged inside the pipe in such a way that it could be moved in a radial direction (y coordinate) as well as in a circumferential direction (φ coordinate). The wire axis was aligned in the circumferential direction. A DANTEC measuring bridge was employed for the hot-wire measurements. The typical sampling rate was 2,000 Hz, and 30,000 samples were recorded. Consequently, the averaging time was 15 s. For a larger amount of samples (2^{20}=1,048,576) and higher sampling rate (31,250 Hz), where the averaging time was about 34 s, no significant changes were observed.

The inside of the pipe was coated with two pieces of special riblet film (see Fig. 5) on a length of 200 mm. The probe was positioned 29 mm upstream of the end of the special film, i.e., the fluid flows above the riblet patterns over a length of Δx=171 mm ($\Delta x/R \approx 2.4$ with pipe radius R=70 mm). Upstream of the films, the pipe was hydraulically smooth. With a centerline velocity U_c=56 m/s, the friction velocity of $U_{\tau,s}$ =1.88 m/s was determined for the smooth wall. (The subscript "s" represents the value of the smooth wall.) The riblet height h and the riblet spacing s (see Fig. 5) are $h^+=s^+=19$, expressed in wall units with $h^+ = hU_{\tau,s}/\nu$, where ν is the kinematic viscosity. The ratio of riblet height to pipe diameter is h/D=152 μm/140 mm≈ 1/1000. As the height of the riblets together with the backing material was about 225 μm, the pipe diameter in the riblet section was reduced to D=139.55 mm (measured from the peaks of the riblets), which corresponds to a reduction in pipe diameter of about 0.3%.

The riblet films were arranged obliquely, with a yaw angle γ=–45° in one half of the pipe and γ=+45° in the other. At the edges of both films, two "V"-shape patterns occurred (see Fig. 6), a convergent riblet pattern at φ=156° and a divergent riblet pattern at φ=336°. Figure 7 shows a

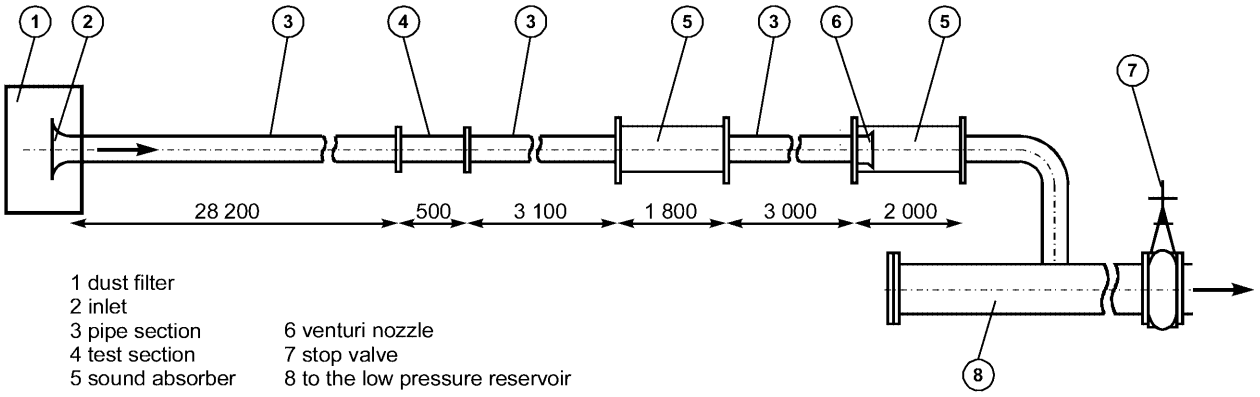

Fig. 4. Sketch of the pipe channel (all measures in mm)

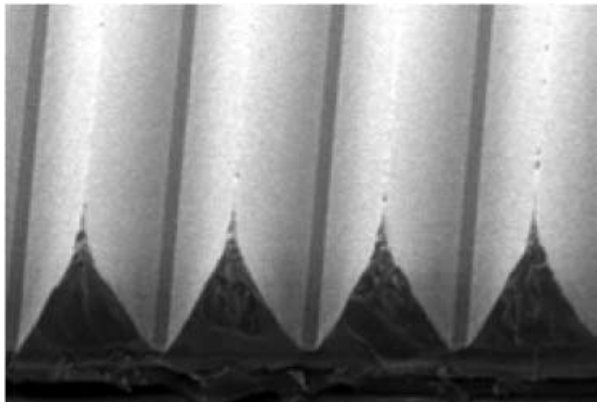

Fig. 5. Special film with V riblets; riblet height h is equal to the riblet spacing s; h=s=152 μm; thickness of the backing material of the riblets sheet is about 75 μm (3M, St. Paul, Minn., USA)

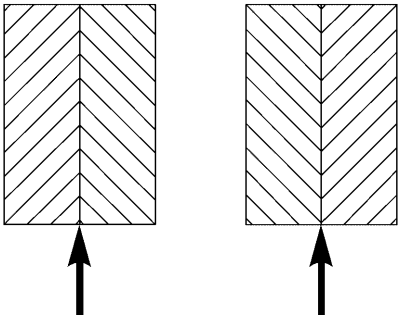

Fig. 6. Arrangements of riblets. Arrows show the flow direction. *Left* – convergent riblet pattern. *Right* – divergent riblet pattern

sketch of both the divergent and the convergent riblet patterns inside the pipe.

3 Experimental results

With convergent and divergent riblet patterns, considerable changes in the flow field close to the wall can be created. Figure 8 shows measurements made near the edges of the films in three different wall distances as a function of the circumferential angle φ. The main results are:

1. It was found that the mean flow velocity U is reduced above the convergent riblet pattern (here at a circumferential angle φ=156°) and that U is increased above the divergent riblet pattern (at φ=336°).
2. The opposite is valid for the velocity fluctuations u_{RMS}: they are higher in the area of the convergent riblet pattern and lower in the area of the divergent riblet pattern. The changes in U as well as in u_{RMS} amount to about 15% as compared to the values measured in the surrounding area.
3. The results described in (1) and (2) can be interpreted clearly: the convergent riblet pattern moves slower fluid material coming from near the wall to the line at φ=156°. This material has to move away from the wall because of continuity. Thus a local decrease in U and an increase in u_{RMS} is observed. This phenomenon is inverse for the divergent riblet pattern: it transports fluid material away from the line at φ=336°. Because of continuity, the fluid material has high velocity, and little disturbance flows towards the wall, causing the local increase of U and at the same time a decrease in the turbulent fluctuations u_{RMS}.

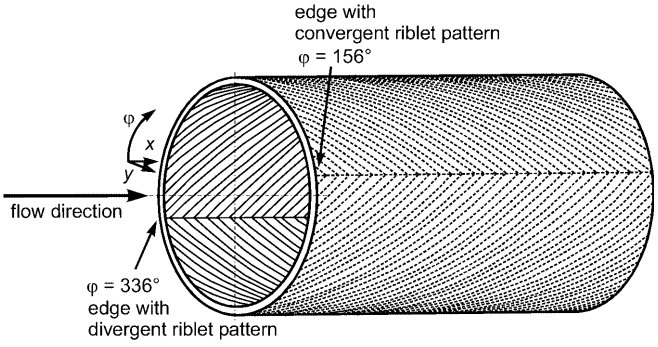

Fig. 7. Divergent and convergent riblet patterns inside the pipe channel

4 Discussion

1. As can be seen from Fig. 8 the values of U and u_{RMS} deviate significantly from their surrounding. The deviation extends in the circumferential direction over about 10 angular degrees ($\Delta\varphi$=10° corresponds to Δz=12 mm or Δz^+=1,500). The measurements were

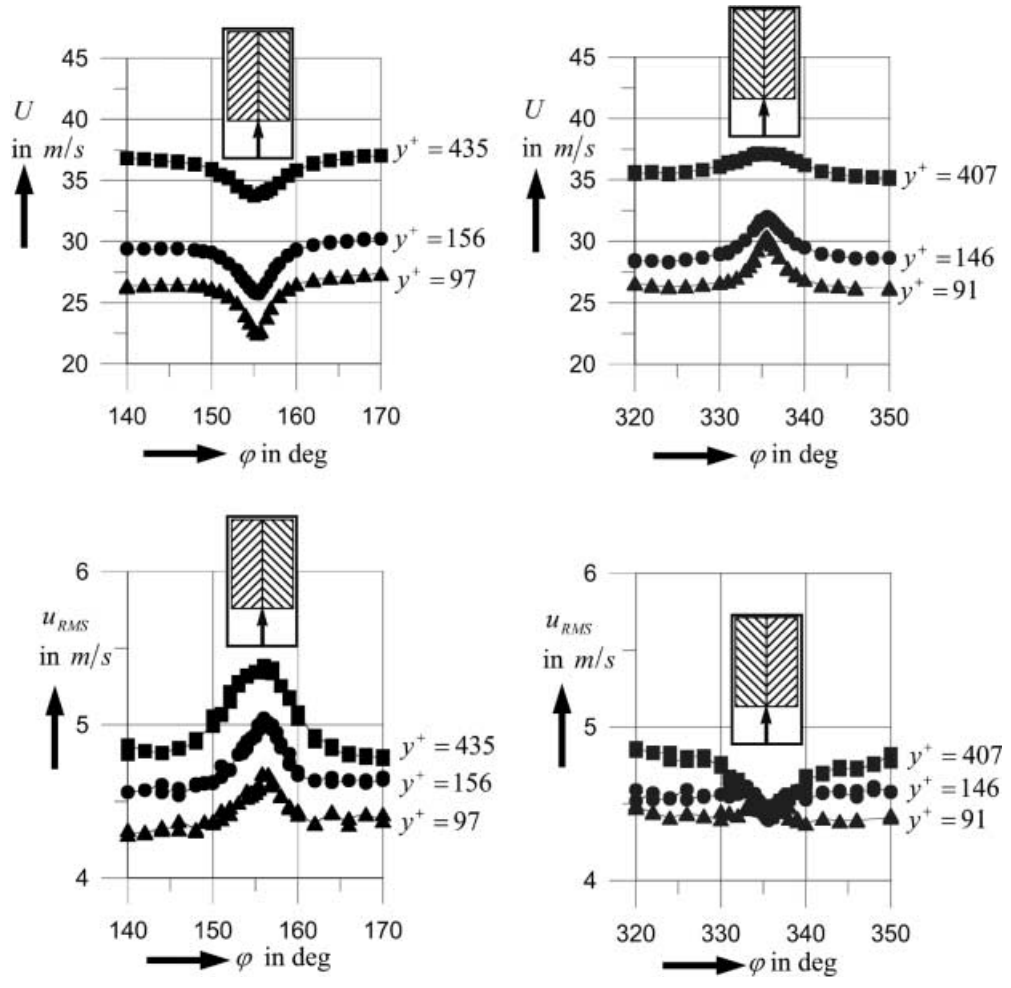

Fig. 8. Time-averaged velocity U (*upper*) and velocity fluctuations u_{RMS} (*lower*) as a function of the circumferential angle φ in the pipe (*left* – convergent; *right* – divergent) in three wall distances $y^+ = yU_{\tau,s}/\nu$ (where y is the distance of the friction velocity above the smooth wall, U_c=56 m/s is the centerline velocity, Re_D=520,000 is the Reynolds number based on pipe diameter , and Re_θ=21,000 is the Reynolds number based on momentum defect thickness)

performed at a position Δx=171 mm, measured from the beginning of the riblet section. It was expected that the process leading to these results developed along the riblet section. In other words, the flow inside the riblet section is not in equilibrium, but depends on Δx. For Δx<171 mm, the influence of the riblets is smaller, as compared to Fig. 8. For Δx>171 mm, the influence was expected to be larger, and it is evident that this effect would not end with the end of the riblet section, but would be maintained over some distance into the smooth walled pipe downstream of the riblet section.

2. The results reported here open new possibilities of influence near wall flows. For example, one can imagine inducing vortices into a flow field or constructing a wall microphone with low aerodynamic background noise.
3. The decreasing turbulent disturbance at divergent riblet patterns measured here coincides with shark-skin observations. As it has already been reported, the skin (the scales) of fast swimming sharks are covered with small riblets. In most cases, the direction of the riblets is in accordance with the flow direction. However, there are areas with divergent riblets. These areas are located upstream of the pores of the so-called lateral-line organ (see Fig. 3). This organ resembles the human ear. In an early paper (Dinkelacker et al. 1988) the authors made the assumption that sharks reduce the local flow noise at the lateral-line organ with the help of these divergent riblet patterns and thereby improve their hearing ability.
4. With respect to quantitatively evaluating the measurements of Fig. 8, one should be aware that the hot wire used is comparatively long (l_{wire}=1.25 mm corresponds to l_{wire}+160, hence very small-scale turbulence is averaged out at the wire) and that the mean velocity in the riblet section is not strictly parallel to the pipe axis. Both effects are not regarded as significant with respect to the results reported here.

5 Conclusions

Close to the wall, the convergent and divergent riblet patterns show considerable differences with regard to the time-averaged streamwise velocity U and the streamwise velocity fluctuations u_{RMS}. If the riblets converge, the time-averaged velocity decreases, and the velocity fluctuations increase. The opposite is found for divergent riblet patterns: here the time-averaged streamwise velocity increases, and the streamwise velocity fluctuations decrease. Near the wall, changes of the local time-averaged velocity and the velocity fluctuations up to ±15% were measured. The application of convergent and divergent patterns of wall riblets opens new possibilities to influence near wall

flows. Further investigations on this topic seem to be worthwhile.

References

Bechert DW, Bruse M, Hage W, Van der Hoeven JGT, Hoppe G (1997) Experiments on drag-reducing surfaces and their optimization with an adjustable geometry. J Fluid Mech 338:59–87

Bechert DW, Hoppe G, Reif WE (1985) On the drag reduction of the shark skin. AIAA Shear Flow Control Conference, 12–14 March 1985, Boulder, Colorado. AIAA 85-0546, pp 1–18

Blackwelder RF, Eckelmann H (1979) Streamwise vortices associated with the bursting phenomenon. J Fluid Mech 94:577–594

Ching CY, Parsons BL (1999) Drag characteristics of a turbulent boundary layer over a flat plate with transverse square grooves. Exp Fluids 26:273–275

Choi H, Moin P, Kim J (1993) Direct numerical simulation of turbulent flow over riblets. J Fluid Mech 255:503–539

Coustols E (1989) Behavior of internal manipulators: "riblet" models in subsonic and transonic flows. AIAA Paper 89-0963, March 1989

Coustols E, Costeix J (1988) Turbulent boundary layer manipulation in zero pressure gradient. In: International Conference on Atomic spectroscopy, ICAS and AIAA. ICAS 88-3.7.3, pp 999–1013

Coustols E, Savill AM (1992) Turbulent skin friction drag reduction by active and passive means – 1 and 2. In: Special course on skin friction drag reduction. AGARD R-786, AGARD, Neuilly-sur-Seine, France, pp 8/1–8/80

Dinkelacker A (1993) Verwendung feiner Wandrillen als Hilfsmittel zur Beeinflussung der Strömungsrichtung in Wandnähe. In: Zukünftige Technologien – Band 4: Bionik. VDI Technologiezentrum, Düsseldorf, pp 78–82

Dinkelacker A, Nitschke-Kowsky P, Reif W-E (1988) On the possibility of drag reduction with the help of longitudinal ridges in the walls. In: Liepmann HW, Narasimha R (eds) Turbulence management and relaminarisation, IUTAM Symposium, Bangalore, India, 1987. Springer, Berlin Heidelberg New York, pp 109–120

Enyutin GV, Lashkov Yu A, Samoilova NV, Fadeev IV, Shumilkina EA (1991) Influence of downwash on the aerodynamic efficiency of fine-ribbed surfaces. Fluid Dynam 26:31–35

Gao X, Sunden B (2001) Heat transfer and pressure drop measurements in rib-roughened rectangular ducts. Exp Thermal Fluid Sci 24:25–34

Gaudet L (1989) Properties of riblets at supersonic speed. Appl Sci Res 46:245–254

Goldstein D, Handler R, Sirovich L (1995) Direct numerical simulation of turbulent flow over a modelled riblet covered surface. J Fluid Mech 302:333–376

Hage W, Bechert DW, Bruse M (1999) Cross-flow effects on optimized riblets. In: Chára Z, Pollert J (eds) Proceedings of the 11th European drag reduction working meeting, 15–17 September 1999, Prague, Czech Republic, p 66

Hage W, Bechert DW, Bruse M (2000) Yaw angle effects on optimized riblets. Notes Numer Fluid Mech 76:278–285

Hirschel EH, Thiede P, Monnoyer F (1988) Turbulence management – applications aspects. Paper presented at the AGARD Symposium on Fluid dynamics of three-dimensional turbulent shear flows and transition, CP-438, Munich, FRG, 3–6 October 1988. AGARD, Neuilly-sur-Seine, France, pp 23/1–23/12

Kim J, Moin P, Moser R (1987) Turbulence statistics in fully developed channel flow at low Reynolds number. J Fluid Mech 177:133–166

Kruse J (1994) Beeinflussung der Grenzschichtströmung eines rotationssymmetrischen Körpers durch Rillenfolien. Diplomarbeit. Georg-August-Universität Göttingen, Institut für Angewandte Mechanik und Strömungsphysik

Lee S-J, Lee S-H (2001) Flow field analysis of a turbulent boundary layer over a riblet surface. Exp Fluids 30:153–166

Reif W-E, Dinkelacker A (1982) Hydrodynamics of the squamation in fast swimming sharks. Neue Jahrb Geol Paläontol Abhandl 164:109–120

Savill AM (1986) Effects on turbulent boundary layer structure of longitudinal riblets alone and in combination with outer layer devices. In: Veret C (ed) Flow Visualization – IV. The Proceedings of the Fourth International Symposium on Flow Visualization, 26-29 August 1986, Ecole Nationale Superieure de Tecniques Avancees, Paris. Hemisphere, New York and Springer, Berlin Heidelberg New York, pp 303–308

Schneider M, Dinkelacker A (1993) Drag reduction by means of surface riblets on an inclined body of revolution. In: Speziale CG, Launder BE (eds) Near-wall turbulent flows. Elsevier, Amsterdam, pp 771–780

Schwarz van Manen AD (1992) Coherent structures over grooved surfaces. PhD thesis, Department of Electrical Engineering, Technische Universiteit Eindhoven, The Netherlands

Squire LC, Savill AM (1987) Some experiences of riblets at transonic speeds. In: Proceedings of the International Conference on Turbulent drag reduction by passive means, 15-17 September 1987, Royal Aeronautical Society, London, UK. European Office of Aerospace Research and Development (EOARD), London, pp 392–407

Walsh MJ (1982) Turbulent boundary layer drag reduction using riblets. AIAA Paper 82-0169

Walsh MJ (1990) Riblets. In: Bushnell DM, Hefner JN (eds) Viscous drag reduction in boundary layers. Progr Astron Aeron 123:203–261

Walsh MJ, Lindemann AM (1984) Optimization and application of riblets for turbulent drag reduction. Presented at the AIAA 22nd Aerospace sciences meeting, 9–12 January 1984, Reno, Nevada. AIAA Paper 84-0347, pp 1–10

Walsh MJ, Weinstein LM (1978) Drag and heat transfer on surfaces with small longitudinal fins. AIAA Paper 78-1161